17th World Conference on Earthquake Engineering, 17WCEE
Sendai, Japan - September 13th to 18th 2020
Paper N° C000830
Registration Code: A00618

DESIGN AND PERFORMANCE OF FRAMES WITH INTENTIONALLY ECCENTRIC BRACES

A. González Ureña[1], R. Tremblay[2], C. A. Rogers[3]

[1] *Ph.D. candidate, Department of Civil Engineering and Applied Mechanics, McGill University, andres.gonzalezurena@mcgill.ca*
[2] *Professor, Department of Civil, Geological and Mining Engineering, Polytechnique Montréal, robert.tremblay@polymtl.ca*
[3] *Professor, Department of Civil Engineering and Applied Mechanics, McGill University, colin.rogers@mcgill.ca*

Abstract

Concentrically Braced Frames (CBFs) with Hollow Structural Sections (HSSs) as the bracing members present significant shortcomings that pose limits to their convenience. Due to their inherently stiff nature, CBFs are usually constrained to low fundamental periods of vibration and, thus, high acceleration and force demands, which, in conjunction with the intrinsic overstrength that derives from the compression resistance controlling the dimensioning of the bracing members, results in high design forces for the capacity-protected components of the structure and its foundations. Furthermore, their ductility and energy dissipation capacity are hindered by the susceptibility of HSSs to low-cycle fatigue induced premature fracturing at the plastic hinge region after the onset of local buckling. To address these shortcomings of Conventional Concentric Braces (CCBs), researchers from Japan recently proposed the use of Braces with Intentional Eccentricity (BIEs). Being subject to both flexural and axial deformations under axial loading, BIEs are inherently less stiff than CCBs. Moreover, their axial stiffness can be adjusted by varying the eccentricity to obtain the desired frame response. Also, initiation of local buckling occurs at larger axial displacements because the strain demand is more evenly distributed over the brace length. However, BIEs are not well suited for standard force-based design procedures given that the force they develop varies continuously with their axial deformation, and that they attain their maximum capacity at large deformation values that depend on the eccentricity. For this reason, the use of BIEs compels the use of an alternative design approach that handles explicitly their particular response to loading.

This article presents a Direct Displacement-Based Design (DDBD) procedure for the seismic design of Frames with Intentionally Eccentric Braces (FIEBs). The proposed procedure includes provisions aiming to control the performance of the structure when subjected to design level earthquakes and to minimize its damage under frequent earthquakes. The method is applied to prototype buildings of 4, 8 and 12 storeys, with square HSS bracing members, and considering two levels of target drift ratio. The structures are designed for a region of high seismic hazard and for a region of moderate seismic hazard, both within Canada. The performance of the so designed buildings is then evaluated through Non-Linear Response-History Analysis (NLRHA). The results show that the seismic performance of FIEBs is satisfactory and on par with the performance objectives incorporated in the procedure and those of the National Building Code of Canada. Furthermore, the resulting tonnage of the FIEB buildings is compared to that of traditional Moderately Ductile and Limited Ductility CBFs designed for identical conditions, showing that FIEBs may constitute an economically advantageous alternative to conventional CBFs, specially in the case of moderately tall buildings located in regions of high seismic hazard.

Keywords: steel braced frames; eccentric braces; earthquake-resistant design; displacement-based design

1. Introduction

Despite their popularity as Seismic-Force Resisting Systems (SFRSs) for low- and mid-rise buildings in seismic regions, due to their efficiency and aesthetic appeal, Concentrically Braced Frames (CBFs) with Hollow Structural Sections (HSSs) as the bracing members bear notable shortcomings that weigh on their overall convenience. To begin with, due to their intrinsic stiffness, CBFs generally possess low fundamental vibration periods, and are thus subjected to high spectral acceleration demands, which, in combination with the considerable overstrength that originates from the compression resistance governing the sizing of the bracing members, leads to large capacity-based design forces for the protected components of the SFRS and foundations, increasing the cost of the structure. In addition to this, HSSs have been proven to be prone to low-cycle fatigue induced fracturing in the mid-length plastic hinge region following the onset of local buckling [1, 2], diminishing their ductility under cyclic loading and their energy dissipation capacity. Lastly, because of the nearly null post-yielding stiffness of Conventional Concentric Braces (CCBs), CBFs are at risk of becoming unstable when subjected to ground motions inducing very large displacement demands or ratcheting.

In 2017, Skalomenos et al. [3] proposed to introduce an intentional eccentricity to otherwise conventional bracing members, addressing the drawbacks stated above by modifying the force-deformation response of the lateral load carrying system. The proposed Braces with Intentional Eccentricity (BIEs) are otherwise regular CCBs, with their longitudinal axis translated with respect to the working points. In contrast with CCBs, BIEs are naturally less stiff as they are subjected to bending moment in combination with axial force. Under tension, they display a pseudo tri-linear force-deformation response with considerable post-yielding stiffness. Under compression, they exhibit a smooth flexural response in which the brace transitions from the elastic to the post-buckling regime without showing sharp peaks due to buckling. Moreover, by adjusting the magnitude of the eccentricity, the pre- and post-yielding stiffness of the BIE can be controlled. Skalomenos et al. performed physical tests under cyclic loading on reduced scale round HSS BIE specimens with two levels of eccentricity. In addition to confirming the behaviour described above, their results showed that, compared to a CCB made from the same HSS, BIEs develop local buckling at the mid-length plastic hinge region at higher imposed drift ratios, thus delaying fracture.

In an effort to reconcile the Capacity-Based Design philosophy that prevails in many modern design codes, such as the National Building Code of Canada [4], and the distinct force-deformation response of BIEs, which sets them apart not only from CCBs, but from most other traditional ductile dissipative elements, the authors of this article propose a design procedure for Frames with Intentionally Eccentric Braces (FIEBs) based on the Direct Displacement-Based Design (DDBD) method. This design approach addresses explicitly the particularities of BIEs, and incorporates provisions aiming to guarantee that the components of the SFRS, other than the braces proper, withstand undamaged the demands arising from the inelastic response of the latter. This paper includes a brief overview of the characteristics of BIEs and their implications on building design, a delineation of the proposed design procedure, and the assessment, through Non-Linear Response-History Analysis (NLRHA), of the performance of twelve example buildings with square HSS BIEs, designed using such procedure.

In a companion paper [5], the authors present results from a numerical parametric study on BIEs, in which some of the herein proposed design procedure's considerations, regarding fracture life and equivalent damping ratios of BIEs, are based.

2. BIEs and their force-deformation response

The components of a nonspecific BIE are presented schematically in Fig. 1. The prescribed eccentricity, e, is the offset between the working points, which generally would coincide with the braced bent diagonal, and the bracing member's axis. The eccentric condition of the brace is achieved by means of *eccentering* assemblies, that is, any sort of plate assembly conceived to transfer rigidly the forces between the bracing member and its connections to the frame, while accommodating the eccentricity. Assuming that the connections at the ends of the BIE behave as pins, its force-deformation response depends on the geometry of the cross-section, the total length, L, the *eccentering* assembly's length, L_{ea}, and the eccentricity.

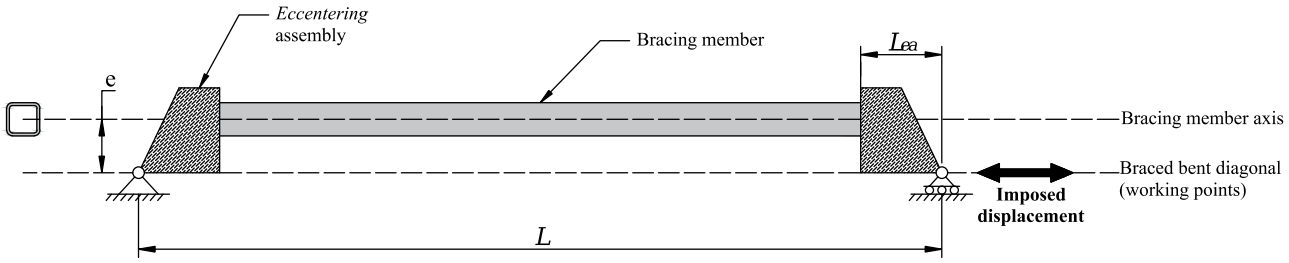

Fig. 1 – Schematic drawing of a general BIE and its components

In Fig 2, the idealised force-deformation behaviour of BIEs under tensile and compressive loads is presented and compared to that of CCBs. Under tensile load, as the BIE elongates it is also subjected to moment and thus bends toward the working point axis. When the outermost fiber in tension reaches the yield stress, the BIE attains the *first yield point*, (T_Y, δ_Y), marking the transition from the elastic to the post-yielding stages, and a net reduction of the stiffness. As loading progresses beyond this point, plastification of the cross-section progresses gradually. However, since the net eccentricity reduces in the deformed configuration of the brace, this stage is characterised by a continuously increasing stiffness. When the complete cross-section reaches yielding, the BIE attains its *ultimate yield point*, (T_U, δ_U), at a force level equal to the yield tensile strength of a CCB. As shown in Fig. 2-(a), the force-deformation behaviour of BIEs in tension can be approximated by a tri-linear model, with an initial, or elastic, stiffness K_i, a secondary, or post-yielding stiffness K_s, and finally, a negligible fully-yielded stiffness.

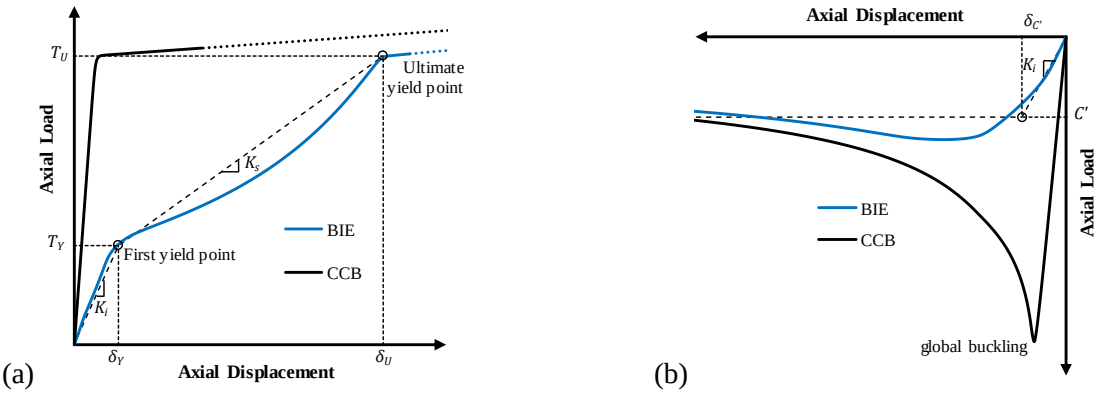

Fig. 2 – Idealised force-deformation behaviour of BIEs and CCBs: tension, (a), and compression, (b)

Under compressive load, the BIE bends away from the working points axis, producing a progressive increment of the net eccentricity and, therefore, a reduction of the stiffness, transitioning seamlessly from the elastic to the post-buckling regime (Fig. 2-(b)). It is proposed that the response of BIEs in compression be approximated with an elastic-perfectly plastic model, with initial stiffness K_i and maximum force, C'. The compressive resistance of the BIE, C', can be estimated, as proposed by Skalomenos et al. [3], by the load corresponding to the elastic limit state of a column under eccentric axial load.

Keeping all other parameters constant, the magnitude of the eccentricity controls the values of T_Y, K_i, K_s, and C'. An example of the influence of the eccentricity on the tensile response of BIEs is presented in Fig. 3, which shows the force-deformation curves in tension of HSS 178×178×16 BIEs for increasing levels of eccentricity, as obtained from OpenSees [6] models. In these models, L was 5408 mm and the *eccentering* assemblies were represented by rigid links with length, L_{ea}, of 360 mm. The end connections were modelled as rectangular plates with thickness of 38.1 mm and width of 360 mm, and a free length of 77 mm intended to yield in flexure under low levels of force, thus approximating the desired pin-like behaviour. The yield stress was taken as 345 MPa both for the plates and the HSS.

When subjected to cyclic loading, the contrast between the CCBs' and the BIEs' responses is also striking. Figure 4 shows the storey shear vs. storey drift plots for pairs of HSS 178×178×16 BIEs, with

eccentricities of 120 and 180 mm acting together opposed against each other, on adjacent 6 m by 4 m braced bays under cyclic load with increasing displacement amplitude, as also obtained from OpenSees analyses. Although, evidently, the force opposed by the BIEs, and the net amount of energy they dissipate, is lower than for CCBs, it is noteworthy that BIEs exhibit a stable hysteretic response with significant positive secondary stiffness. The absence of peaks due to buckling would allow for avoiding the requirement of considering separate buckling and post-buckling cases when determining the capacity-based demands on the protected elements.

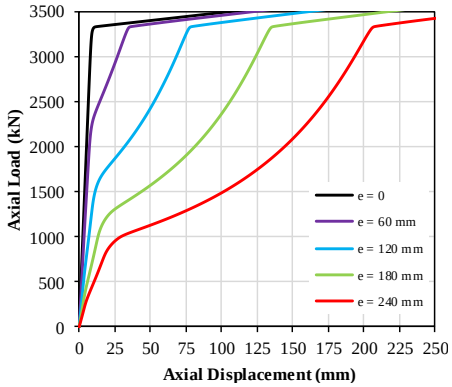

Fig. 3 – Influence of eccentricity in the tension force-displacement behaviour of 178×178×16 HSS BIEs

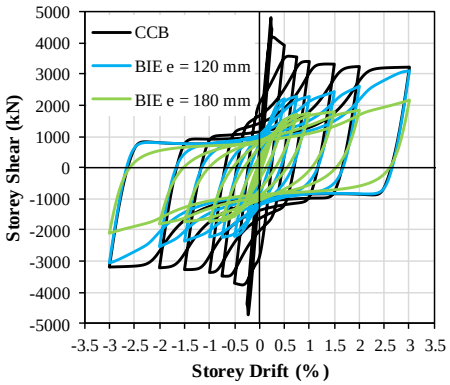

Fig. 4 – Storey shear vs. drift for 6 m by 4 m bays braced with 178×178×16 HSS BIEs and CCBs

3. Proposed design procedure for FIEBs

As can be implied from the previous section, force-based procedures, commonly employed following up-to-date code provisions, such as those provided in [4] for the design of MD-, LD- and CC-CBFs, are not well suited for use in the design of FIEBs. Standard force-based design procedures, albeit implicitly, assume that the dissipating elements behave in an elastic-perfectly plastic manner, with small yield displacements or rotations. This allows for the dissipating elements to be dimensioned by leveling their capacity to the anticipated seismic force demands, scaled down in account of the ductility and overstrength of the system. In the case of BIEs, however, the maximum force level depends on the eccentricity, and the associated axial displacement can often be too large to be compatible with serviceability limit states, rendering inappropriate an approach based on said maximum force. Furthermore, their post-yielding stiffness is not negligible and, as stated earlier, will increase with the displacement (Fig. 2-a); as such, their overall force-deformation response strays far from an elastic-perfectly plastic idealisation.

Considering the arguments above, and noting that for a given section and set of dimensions, the relevant properties of the BIEs' response for design effects (i.e. T_Y, T_U K_i, K_s, and C'), can be easily obtained numerically for any eccentricity value, thus enabling to express the force developed as a function of the imposed displacement, the adoption of a displacement-based design procedure appears as an appropriate course of action for FIEBs. More precisely, a procedure based on the Direct Displacement-Based Design (DDBD) [7] is adopted in this research. In the available literature, several examples of the successful application of DDBD to the design of CBFs are available [8, 9]. A preliminary version of the design procedure, and its application to the design of FIEBs, was presented by the authors in [10]. In the following lines, a brief description of the steps constituting the proposed design procedure is presented.

1. *Selection of Target Storey Drift, θ_d, and definition of equivalent SDOF mass and displacement*

The normalised target displacement vector is calculated using Eq. (1), which corresponds to inelastic mode shapes for low-rise and taller moment frames given in [7]. Although expressions developed specifically for CBFs have been proposed [11], verifications performed by the authors indicate that the mode shapes given by Eq. (1) are closer to the inelastic mode shape of FIEBs, presumably owing to their higher flexibility decreasing the contribution of the columns' deformation to the deformed shape. In Eq. (1), n is the number of storeys, H_i

and H_n are the elevations of the i[th] and top storeys, and δ_i is the normalised lateral displacement of the i[th] storey. The normalised target displacement vector is then scaled so that the maximum storey drift matches the Target Storey Drift, θ_d, which corresponds to the maximum storey drift that is intended to occur in the building under the Design Earthquake, and is defined as the starting point of the design process.

$$\begin{aligned} n \le 4: &\qquad \delta_i = \frac{H_i}{H_n} \\ n > 4: &\qquad \delta_i = \frac{4H_i}{3H_n}\left(1 - \frac{H_i}{4H_n}\right) \end{aligned} \tag{1}$$

Having obtained and scaled the normalised displacement vector, the equivalent SDOF mass, M_{eq}, and displacement, Δ_{eq}, can be calculated with Eq. (2) and Eq. (3), where d_i and m_i are the target displacement and the mass of the i[th] storey.

$$\Delta_{eq} = \frac{\sum d_i^2 m_i}{\sum d_i m_i} \tag{2}$$

$$M_{eq} = \frac{\sum d_i m_i}{\Delta_{eq}} \tag{3}$$

2. Determination of the Target Secant Period from the Damped Displacement Design Spectrum

The target secant period, T_{eq}, corresponds to the ordinate of the point with abscissa Δ_{eq} in the Damped Displacement Design Spectrum. To avoid excessively flexible structures, however, the authors recommend that T_{eq} should not be taken larger than 10 s. The 5 % damped displacement spectrum, S_d, can be obtained directly from the design acceleration spectrum, S_a, using Eq. (4), and the be scaled down to account for the equivalent viscous damping, ξ_{eq}. In this research, the equivalent damping reduction factor, R_ξ, recommended by Eurocode 8 [12], given by Eq. (5), is adopted.

$$S_d = S_a \frac{T^2}{4\pi^2} \tag{4}$$

$$R_\xi = \sqrt{\frac{0.1}{0.05 + \xi_{eq}}} \tag{5}$$

The proper ξ_{eq} value to be used depends on the sections selected for the BIEs and on their anticipated ductility demand. As is explained in the companion paper [5], the model developed by Wijesundara et al. for CCBs [13], given in Eq. (6), is used in this research. At the beginning of the design process, the BIEs' sections are not known and it is suggested to use ξ_{eq}= 0.15 as an initial estimate, to be corrected or verified later on. In Eq. (6), μ is the ductility demand on the BIE, calculated with respect to its first yield point, r is the section's radius of gyration and E is the modulus of elasticity.

$$\begin{aligned} \mu \le 2: &\qquad \xi_{eq} = 0.03 + \left(0.23 - \frac{\lambda}{15}\right)(\mu - 1) \\ \mu > 2: &\qquad \xi_{eq} = 0.03 + \left(0.23 - \frac{\lambda}{15}\right) \\ &\qquad \lambda = \frac{L}{r}\sqrt{\frac{F_Y}{\pi^2 E}} \end{aligned} \tag{6}$$

3. Calculation of target "primary" secant stiffness, base shear, and equivalent static force vector

Having determined T_{eq}, the target "primary" secant stiffness, K_{eq}, can be obtained from Eq. (7). This stiffness, directly related to the target spectral displacement of the equivalent SDOF system, is dubbed "primary" to be put in contrast with additional, "auxiliary" stiffness that the FIEB may require to fulfill stability and regularity

criteria, as will be explained. With K_{eq}, the equivalent "primary" base shear is obtained through Eq. (8), and then distributed to each storey using Eq. (9) and Eq. (10), which are taken from [4].

$$K_{eq} = 4\pi^2 \frac{M_{eq}}{T_{eq}} \tag{7}$$

$$V_{eq} = K_{eq}\Delta_{eq} \tag{8}$$

$$F_{eq,i} = (V_{eq} - F_t)\frac{W_i h_i}{\sum_{i=1}^{n} W_i h_i} \tag{9}$$

$$F_t = 0.07 T_{eq} V_{eq} < 0.25 V_{eq} \quad (\text{for } T_{eq} > 0.7 \text{ s}) \tag{10}$$

4. Selection of BIEs for each storey

At each storey, the BIEs are selected in terms of section-eccentricity pairs, e.g. HSS 152×152×13 – e = 140 mm, such that the net lateral force they produce at the design displacement is equal to than the *design shear*, while complying with minimum stiffness, regularity, serviceability and fracture life criteria hereon discussed. The storey *design shear*, $v_{d,i}$, calculated with Eq. (11) is defined as the sum of the equivalent "primary" storey shear $v_{eq,i}$ and the notional loads, $v_{n,i}$, (taken as 0.005 times the factored gravity loads as per [4]), amplified by the factor $U_{2,i}$ given by Eq. (12). The $U_{2,i}$ factor, taken from CSA S16-14 [14], is used to include the estimated P-Δ effects expected at the level of the design displacements. In Eq. (12), $C_{f,i}$ are the cumulated factored gravity loads at the i[th] storey and v_i^* is the storey shear provided by the selected BIEs at the design displacement level.

$$v_{d,i} = U_{2,i}(v_{eq,i} + v_{n,i}) \tag{11}$$

$$U_{2,i} = 1 + \left(\frac{C_{f,i} d_i}{v_i^* h_i}\right) \tag{12}$$

Aiming to prevent potential instability issues, it is recommended that the ratio of secant lateral stiffness to geometric negative stiffness be larger than 1.5 at every storey. To further favour an adequate response of the structure, i.e. to avoid large concentrations of demands in particular storeys, the vertical stiffness regularity criterion of NBCC 2015 [4] is observed.

Recognizing that BIEs may have first yield points markedly lower than the yield strength of other, conventional, dissipating elements, and that premature yielding under frequent loading conditions is undesirable, the design procedure suggests that in each storey, the shear resistance that the selected BIEs can provide within the elastic range, i.e. that associated with axial forces equal to C' in both the tension and compression braces, be at least equal to the larger between the equivalent static storey shear calculated for a frequent, or service level, earthquake, which for the purposes of this research is determined using the acceleration spectra for a probability of exceedance of 40 % in 50 years, and the factored wind shear. The elastic, or initial, period of the FIEB, T_i, used in the calculation of the considered frequent earthquake can be conservatively estimated using Eq. (13).

$$T_i = 0.05 H_n \tag{13}$$

Finally, the fracture life of the selected BIEs shall be estimated in order to select section-eccentricity pairs that can indeed attain safely the intended displacement levels under cyclic loading. This can be performed using the proposed expression for the allowable drift ratio, θ_{md}, whose development is explained in the companion paper [5], and is given by Eq. (14), where e_0 is the ratio of the eccentricity to the HSS outside height and $\lambda_0 = \frac{Lt}{rb_{el}}$ is a combined slenderness parameter (t is the HSS thickness and b_{el} is the effective width of its walls).

$$\theta_{md} = -0.4312 + 0.1943\lambda_0 + 0.6704 e_0 - 0.001319\lambda_0^2 - 0.01833\lambda_0 e_0 + 0.241 e_0^2 \tag{14}$$

To expedite the selection of the section-eccentricity pairs at each storey, is it suggested to assemble beforehand a database of BIE properties considering the available sections, a wide range of eccentricities, and the actual dimensions that the BIE would have when installed in the braced bay. This way, the forces that the BIEs develop as a function of the imposed displacement will be readily available and all the verifications included in the design procedure can be easily performed in a spreadsheet. The BIE properties can be easily gathered using fiber-based models in OpenSees, considering nominal material properties.

5. *Design of the capacity-protected elements of the FIEB*

In order to provide the conditions for the FIEBs to be able to develop their expected force-deformation hysteretic response at the design level, or eventually beyond, the non-dissipating elements of the FIEB are deemed protected members and designed according to Capacity-Based Design principles. Thus, the connections, beams, columns and foundations are dimensioned so that their response is elastic under the demands arising from the inelastic action of the braces. Acknowledging the unavoidable uncertainty in the prediction of the maximum storey drifts, it is proposed that the probable forces exerted by the braces on the protected elements of the FIEB be taken as those corresponding to 1.25 times the design storey drift, considering probable material strength (i.e. $R_Y F_Y$). As discussed above, since the response of the BIEs in compression can be reasonably modelled as elastic-perfectly plastic, there is no need to distinguish between the buckling and post-buckling cases when determining the probable forces imposed in the non-dissipating elements of the FIEB.

6. *Assessment of the performance of the resulting design*

Considering the high degree of non-linearity of the BIEs' response, and that research on the structural system is still incipient, it is recommended that once the design has been completed, the performance of the building be assessed using a detailed analysis such as NLRHA to verify that the performance objectives are met.

4. Seismic Performance of FIEBs

To evaluate results obtained from the application of the proposed procedure, 12 buildings with FIEBs as their SFRS were designed. Two locations within Canada were selected to represent high and moderate seismic hazard: Vancouver, British Columbia, and Montréal, Québec. For each location, 12-, 8- and 4-storey FIEB buildings were designed for two values of θ_d: 2.5 % and 1.5 %. The 2.5 % drift level corresponds to the maximum allowable drift ratio for buildings of the Normal Importance Category as per the NBCC [4], and the 1.5 % target drift was selected as a moderate value to determine the effects of different target drift ratios on the performance and cost of the structures. All buildings were designed for identical dead and live loads, and for the snow and wind loads corresponding to their location. Class C (firm ground) site condition was assumed in all cases for the determination of the acceleration spectra. Square HSSs were considered for the bracing members and CSA G40.21–350W steel material was assumed for all components. A braced configuration consisting of pairs of single diagonals acting in opposite directions in adjacent bays, as shown in Fig. 5, which also presents the plan configuration of the buildings, was selected. The resulting structural design specific to any of the FIEBs along the E-W direction is included herein.

The connections of the braces to the frame consist of gusset- and knife-plate assemblies, connected by bolted angles. The introduction of the eccentricity is achieved by the use of side-plates linking rigidly the HSS to the knife plate, detailed using a clearance with a length of twice the plate's thickness, t_g, to allow for the unrestrained rotation of the BIE's ends. The knife plate is designed to yield in flexure at low levels of load. This configuration was selected because of its simplicity and cost-effectiveness, but also to produce in-plane bending of the frame, thus preventing the storey drifts from imposing flexural demands on the BIEs other than those produced by their eccentricity. The intent was to favour a more predictable force-deformation hysteretic response. A drawing of the typical considered *eccentering* assembly and connection configuration is presented in Fig. 6.

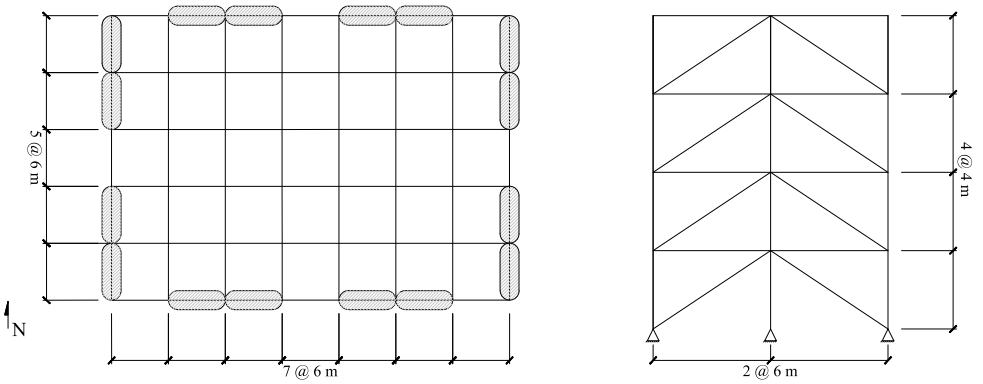

Fig. 5 – Plan configuration of the buildings and elevation of the considered SFRS (4-storey frame shown)

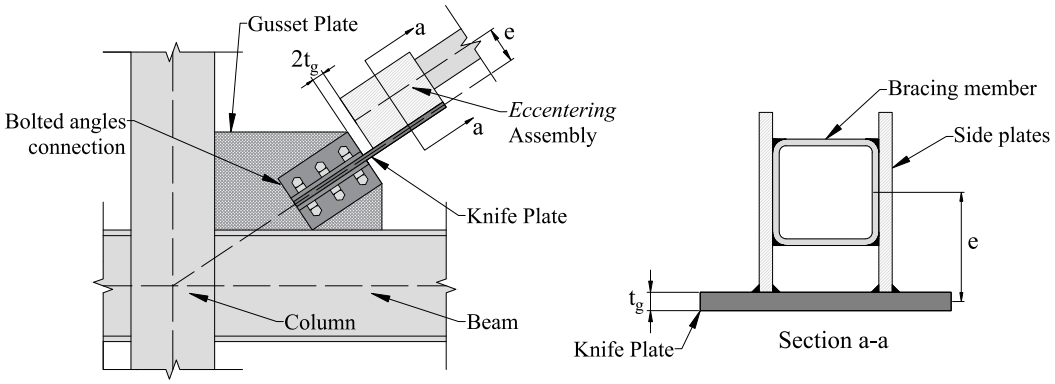

Fig. 6 – Example of the considered BIE to frame connection and *eccentering* assembly

Table 1 presents the target secant periods for the 12 designed buildings, as obtained from Step 2 of the design procedure, as well as the limit state which governed in the selection of the BIEs: Design Earthquake, Service Level Earthquake, or factored wind loading. It can be noted that for the location with moderate seismic hazard (Montréal), the 10 s limit on the target period governed for all buildings, as it did for the 12-Storey FIEB with θ_d= 2.5 % located in Vancouver. It is also worth noting that, in most cases, the Service Level Earthquake equivalent static forces determined the BIE selection, and that in one case the wind loads governed. This implies that the chosen structure provided significantly more stiffness and resistance than that required to meet the intended displacements under the action of the Design Earthquake alone, therefore undermining the relevance of the target drift ratios. An example of the resultant designs is presented in Fig. 7. As can be seen, only two HSS section sizes are used over the building's height, a result of varying the eccentricity introduced by the *eccentering* assembly. It has been found through iteration, that the most efficient design, considering cost and compliance with the design procedure's requirements, is often obtained by selecting one constant brace section for the lower three fourths to two thirds of the structure, and another one for the top storeys.

Table 1 – Target secant period and limit state governing the design of the 12 buildings

	Vancouver		Montréal	
Building type	Target period	Governing limit state	Target period	Governing limit state
12-Storey, θ_d=2.5 %	> 10 s	Service level earthquake	> 10 s	Design earthquake
12-Storey, θ_d=1.5 %	4.98 s	Design earthquake	> 10 s	Design earthquake
8-Storey, θ_d=2.5 %	6.97 s	Design earthquake	> 10 s	Wind
8-Storey, θ_d=1.5 %	3.24 s	Service level earthquake	> 10 s	Service level earthquake
4-Storey, θ_d=1.5 %	3.41 s	Service level earthquake	> 10 s	Service level earthquake
4-Storey, θ_d=1.5 %	1.76 s	Service level earthquake	> 10 s	Service level earthquake

The seismic performance of the FIEB buildings was assessed through NLRHA of models based on fiber elements of the SFRSs in OpenSees. In the models, a yield strength of 460 MPa was considered for the HSSs and of 385 MPa for the beams, columns and connection elements, to represent probable material resistances. P-Δ effects were included in the models by incorporating a leaning column carrying the concomitant gravity loads tributary to the FIEB. For each location, a suite of ground motions specifically selected and scaled to be representative of the seismic hazard at the design level was selected, observing the provisions in [4]. In the case of Vancouver, three suites of five ground motion records were considered for the three seismic sources that contribute to the seismic hazard in that location: shallow crustal earthquakes, deep in-slab subduction earthquakes, and large interface subduction events [15]. For Montréal, a suite composed of 11 synthetic ground motions, developed by Atkinson [16], was selected. Only horizontal acceleration was considered in the analyses.

Additionally, to determine whether the BIEs remained in the elastic range during a service level earthquake, a second round of NLRHA was performed, with the ground motions scaled down accordingly. Scale factors with values of 0.23 and 0.12 were used for Vancouver's and Montréal's ground motion suites, respectively, based on the maximum ratio between the spectral acceleration values of the spectra with 40 % and 2 % probability of exceedance in 50 years. Although this approach is an approximation that does not represent accurately the aggregated seismic hazard for the more frequent earthquakes, its use here to verify whether the BIEs comply with the proposed serviceability condition, may be considered acceptable.

In general, the NLRHA results show that the performance of the FIEBs was satisfactory, although the target drifts were not met: in all cases, the maximum storey drifts for any of the ground motions were significantly lower than the selected target drifts, owing both to the additional strength and stiffness provided to comply with the serviceability condition, and to the upper limit of 10 s applied to the target period. The building for which the maximum storey drifts were closer to the target drifts was the 12-storey Vancouver FIEB with θ_d=1.5 %, seemingly because this was the only building located in the high seismic hazard region for which neither the design level earthquake nor the maximum target period governed the design. As shown in Fig. 8, the 84th percentile value of its maximum storey drifts is close to 1.25 %. As well, it was confirmed that the maximum storey shears were lower than the design probable storey shears used to design the capacity protected elements, which indicates that the related provision fulfills its purpose. An example of this is presented in Fig. 9. From the results of the second round of NLRHA, it was confirmed both that the mean of the maximum storey drifts produced by the scaled-down ground motion suites were for all buildings lower than the storey drifts associated with the maximum storey capacity within the elastic range (elastic limit drifts), and that the residual storey drifts after the earthquake excitation were negligible, suggesting that the proposed design provision helps in assuring that the buildings will not likely be damaged by demands arising from frequent earthquakes or wind loads. The compared maximum storey drifts and elastic limit drifts are shown for the 12-storey FIEB with θ_d=2.5 % in Vancouver in Fig. 10, and Fig. 11 presents the residual storey drifts for the 12-storey FIEB with θ_d=1.5 % in Vancouver. Note that a residual drift of 0.008 % corresponds to an inter-storey displacement of 0.32 mm.

For all Vancouver buildings, it was observed that, for the design ground motion level, the interface subduction earthquakes invariably produced the largest responses, in terms of storey drifts and shears, even for the 4-storey buildings, as shown in Fig. 12. Presumably, this is due to the larger effective periods of FIEBs, in comparison with other systems, such as CBFs. However, as Fig. 11 shows, crustal earthquakes may govern the building's response at the service level earthquake. Furthermore, as can be noted from Figs. 8, 10, 11 and 12, the maximum storey drifts are concentrated in the higher storeys, showing the considerable contribution of the higher mode effects, likely related as well to the increased flexibility of the system. These results showcase one of the limitations of the design procedure as presented here that shall be addressed in future stages of the research through a formal calibration of a target displacement vector better suited for the system.

As shown in Fig. 13, the characteristic force-deformation hysteretic behaviour is recognizable in the storey shear vs. drift history plots obtained under the effects of the imposed ground motions. Two distinct regimes, elastic (or initial) and post-yielding, are clearly marked in the plot and demonstrate the system's property of increasing its resistance and energy dissipation capacity as the displacement demands increase.

Potentially, the significant post-yielding stiffness of BIEs and their increased fracture life, renders FIEBs more apt, in comparison to CCBs, to overcome seismic demands larger than those considered in design.

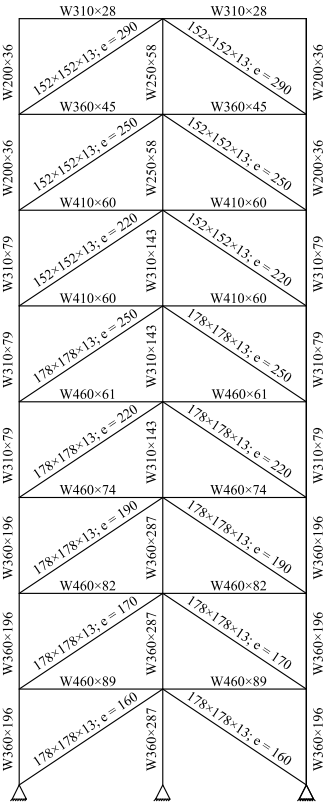

8 Storey FIEB, Vancouver

θ_d= 2.5 %,

Fig. 7 – Example of resulting FIEB design

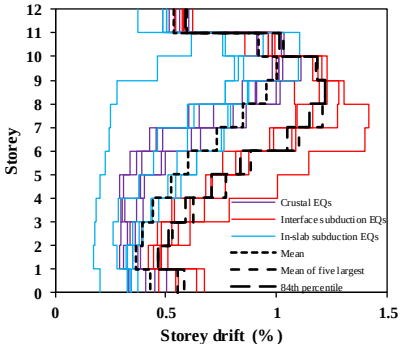

Fig. 8 – Maximum storey drifts for the 12-storey FIEB with θ_d=1.5 % in Vancouver

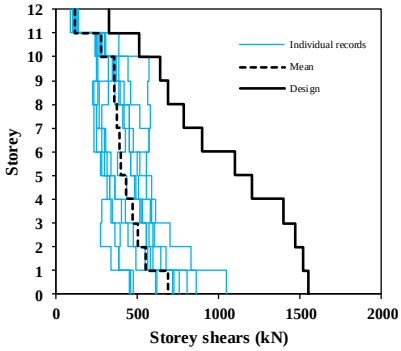

Fig. 9 – Maximum storey shears for the 12-storey FIEB with θ_d=1.5 % in Montréal

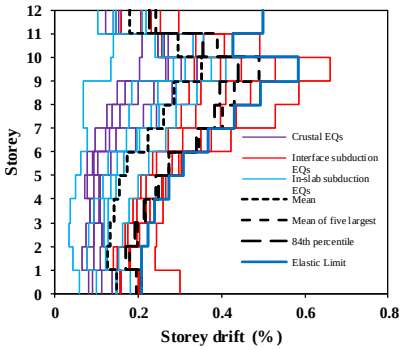

Fig. 10 – Maximum storey drifts for the 12-storey FIEB with θ_d=2.5 % in Vancouver, for scaled-down ground motions

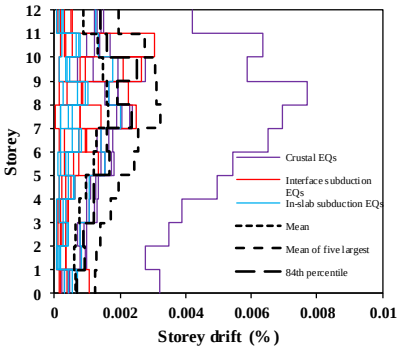

Fig. 11 –Residual storey drifts for the 12-storey FIEB with θ_d =1.5 % in Vancouver, for scaled-down ground motions

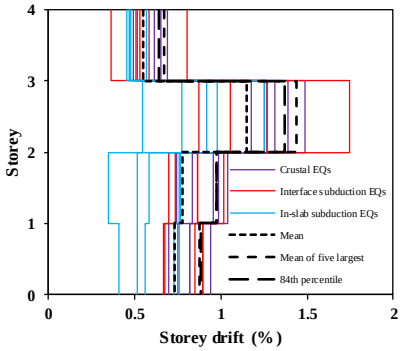

Fig 12 – Maximum storey drifts for the 4-storey FIEB with θ_d=2.5 % in Vancouver

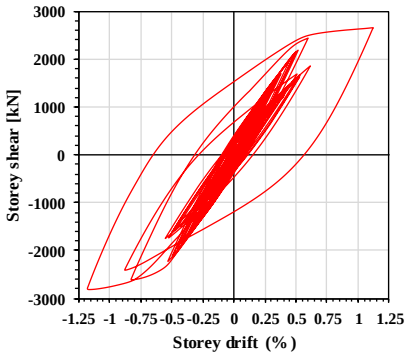

Fig. 13 – Example of first storey shear vs. drift history plot for the 12-storey FIEB with θ_d=2.5 % in Vancouver, subjected to one of the interface subduction ground motions

To allow for a comparison, in terms of net tonnage, of the proposed FIEB system against traditional CBF buildings. Moderately Ductile (MD-) CBF and Limited Ductility (LD-) CBF versions of the buildings were also designed following the provisions from [4]. Although MD-CBFs taller than 40 m are not permitted by the NBCC 2015, the 12-storey CBFs with a height of 48 m, were designed nonetheless to obtain their

hypothetical weight. The results of the tonnage comparison are given in Table 2. As the results show, FIEBs can require significantly less material that conventional CBFs, in particular for the larger building height considered and for the location with high seismic hazard. Although the net weight of the bracing members is greater in the FIEBs, this is compensated by a reduction of the material required for beams and columns due to the lower capacity-based design forces that determine their required dimensions. Had the foundations also been included in the comparison, the differences between the two systems would be more marked. The results also show that there is no recognizable difference between the costs of the FIEBs designed for θ_d=2.5 % and those designed for θ_d=1.5 %. Once more, this is a result of the proposed serviceability conditions and upper limit to the target period governing the selection of the BIEs. If these requirements were not applied, the FIEBs designed for θ_d=1.5 % would have a tonnage approximately 25 % higher, on average, than the ones designed for the larger target drift. However, it is arguably of greater benefit to guarantee that the flexibility of the system is not excessive, that minimum serviceability conditions are satisfied and that the building will respond adequately, i.e. elastically, to the factored wind loads.

Table 2 – Steel tonnage for the resulting designs

	Vancouver			Montréal		
Building type	Beams and columns (ton)	Bracing members (ton)	Total weight (ton)	Beams and columns (ton)	Bracing members (ton)	Total weight (ton)
MD-CBF*	65.74	10.36	76.11	29.54	4.41	33.95
LD-CBF	76.69	10.80	90.49	22.76	4.43	27.19
12-Storey, θ_d=2.5 %	41.53	12.43	53.96	21.92	8.52	30.44
12-Storey, θ_d=1.5 %	43.75	12.09	55.84	21.89	6.95	28.84
MD-CBF	22.76	4.56	27.33	12.87	2.39	15.26
LD-CBF	30.69	6.63	37.31	12.83	3.18	16.01
8-Storey, θ_d=2.5 %	18.69	6.93	25.62	11.34	3.01	14.35
8-Storey, θ_d=1.5 %	19.02	7.23	26.24	11.63	3.00	14.63
MD-CBF	6.53	2.05	8.58	4.85	1.14	5.99
LD-CBF	7.26	2.43	9.70	4.84	1.52	6.35
4-Storey, θ_d=2.5 %	5.92	3.08	8.99	4.63	1.49	6.12
4-Storey, θ_d=1.5 %	6.44	3.14	9.58	4.15	1.26	5.41

5 Conclusions

The characteristics of the force-deformation response of BIEs allow them to overcome some of the most recognisable downsides of CCBs, in particular their invariably high stiffness and their propension to premature fracturing. Acknowledging the incompatibility of the traditional force-based design procedures with the BIEs' response, a seismic design procedure based on the DDBD method and the provisions from the National Building Code of Canada was formulated. It was found that buildings designed with said procedure offered a satisfactory performance, complying with all the selected target maximum drifts and performance objectives, both for the design ground motion and for demands closer to those expected for frequent earthquakes. The results also showed that the use of FIEBs can be advantageous in terms of cost compared to that of CBFs, specially for buildings with more than 8 storeys located in regions of high seismic hazard.

However, the design procedure failed to effectively produce buildings that would meet the intended target displacement levels as it required to provide the structures with additional stiffness and strength in order to fulfill the proposed minimum serviceability criteria. The current state of the design procedure also showed its limitations regarding the estimation of the contribution of the higher mode effects. These shortcomings of the design procedure will be addressed in future stages of the research program. The estimated fracture life of

square HSS BIEs is also to be verified through physical testing under cyclic loading of full-scale specimens with *eccentering* assemblies such as those described above.

6. Acknowledgements

The authors would like to thank DPHV Structural Consultants, ADF Group Inc. and Constructions Proco for their generous technical and financial support, as well as the Natural Sciences and Engineering Research Council (NSERC) of Canada, the Fonds de Recherche du Québec – Nature et Technologies (FRQ-NT) and the Centre d'Études Interuniversitaire des Structures sous Charges Extrêmes (CEISCE). The first author also wishes to acknowledge Universidad de Costa Rica for financing the undertaking of his doctoral studies.

7. References

[1] Tang X, Goel S (1989): Brace fractures and analysis of phase I structure. *ASCE Journal of Structural Engineering*, **115**(8), 1960-1976.

[2] Tremblay R (2002): Inelastic response of steel bracing members. *Journal of Steel Constructional Steel Research*, **58**(5-8), 665-701

[3] Skalomenos K, Inamasu H, Shimada H, Nakashima M (2017): Development of a steel brace with intentional eccentricity and experimental validation. *ASCE Journal of Structural Engineering*, DOI: 10.1061/(ASCE)ST.1943-541X.0001809

[4] NRCC (2015): *National building code of Canada 2015, 14th ed*. National Research Council of Canada, Ottawa, Canada

[5] González Ureña A, Tremblay R, Rogers CA (2020): Numerical investigation of the seismic response of square HSS braces with intentional eccentricity. *17th World Conference on Earthquake Engineering*, Sendai, Japan. Paper nº C000832 (Submitted)

[6] McKenna F, Fenves G, Scott M (2004): *Open system for earthquake engineering simulation*. Pacific Earthquake Engineering Center, University of California, Berkeley, USA

[7] Priestley M, Calvi GM, Kowalsky M (2007): *Displacement-based seismic design of structures.* IUSS Press, Pavia

[8] Wijesundara K, Rajeev P (2012): Direct displacement-based design of steel concentric braced frames structures. *Australian Journal of Structural Engineering*, **13**(3), 243-257

[9] O'Reilly G, Goggins J, Mahin S (2012): Performance-based design of a self-centering concentrically braced frame using the Direct Displacement-Based Design procedure. *15th World Conference on Earthquake Engineering*, Lisbon, Portugal

[10] González Ureña A, Tremblay R, Rogers CA (2019): Design and seismic performance of multi-storey frames with intentionally eccentric braces. *12th Canadian Conference on Earthquake Engineering*, Québec, Canada

[11] Al-Mashaykhi M, Rajeev P, Wijesundara K, Hashemi M (2019): Displacement profile for displacement based seismic design of concentric braced frames. *Journal of Constructional Steel Research*,**155**, 233-248

[12] CEN (2004): *EN 1998-1: 2004 Eurocode 8: Design of structures for earthquake resistance- Part 1: General rules, seismic action and rules for buildings.* European Committee for Standardisation, Brussels, Belgium

[13] Wijesundara K, Nascimbene R, Sulivan T (2011): Equivalent viscous damping for steel concentrically braced frame structures. *Bulletin of Earthquake Engineering.* **9**, 1535-1558

[14] CSA (2014): *CSA S16-14: Design of steel structures.* Canadian Standards Association, Toronto, Canada

[15] Tremblay R, Atkinson GM, Bouaanani N, Daneshvar O, Léger P, Koboevic S (2015): Selection and scaling of ground motion time histories for seismic analysis using NBCC 2015. *11th Canadian Conference in Earthquake Engineering*, Victoria, Canada

[16] Atkinson GM (2009): Earthquake time histories compatible with the 2005 National Building Code of Canada uniform hazard spectrum. *Canadian Journal of Civil Engineering*, **36**(6), 991-1000

